Analysis of Crystallographic High Temperature Fatigue Crack Growth in a Nickel Base Alloy

K. SADANANDA AND P. SHAHINIAN

Crack growth behavior of a nickel-base alloy, Udimet 700, was studied at room temperature and 850 °C in air and vacuum. Crack growth rates were higher in air than in vacuum but this increase in growth rates was nearly the same at both temperatures. In contrast to the effect of environment, an increase of temperature from 25 to 850 °C has a much larger effect on growth rates although the mode of crack growth did not change with temperature or with environment. A detailed analysis of the fracture surfaces indicated that the growth rates under all of the above experimental conditions occurs by a crystallographic faceted mode with the plane of the facet identified to be the {100} cleavage plane rather than a slip plane. Also the increase in growth rates with temperature appears not to be directly related to an environmental effect, creep effect or variation of elastic modulus with temperature.

IT is well known[1] that crack propagation under fatigue generally occurs first by Stage I followed by Stage II. Stage I crack growth is usually limited to one or two grains from the specimen surface and is mostly along slip bands. Therefore, the fracture surface in Stage I tends to have a definite crystallographic orientation. On the other hand, Stage II growth is essentially noncrystallographic and occurs close to the plane of maximum normal stress and is frequently associated with the presence of striations on the fracture surface. Several studies in recent years,[2-17] however, have shown that in high strength materials, particularly those that have propensity for planar slip, fatigue crack growth occurs by a faceted mode with facets showing the features characteristic of cleavage fracture such as river lines. Several terms such as faceted mode, cleavage mode and quasicleavage mode have been used to distinguish this mode of crack growth from the ductile striation mode as well as classical cleavage fracture.

Identification of the plane of the facets with the slip plane of the material in some cases led to the belief that the faceted mode of crack growth in these materials is essentially Stage I mode of crack growth which extends to a large part of the fatigue fracture surface.[8,9] In some other materials,[11,12] facets were along the cleavage planes indicating that fatigue crack growth in these materials occurs by progressive cleavage. In fact, Richards[4] observed that in Fe-3 pct Si the plane of the facets depends on the degree of symmetry of the slip systems with respect to crack plane. Hertzberg and Mills[14] found that faceted mode of crack growth occurs even in relatively ductile materials that have low stacking fault energy and thus restricted cross slip. for these materials, crack growth occurs by a faceted mode particularly at low ΔK values close to the threshold stress intensity range but changes to the ductile striation mode at high ΔK values. Most of the experimental observations, however, have been limited to room temperature. In the present analysis, this mode of fatigue crack growth is examined in detail at different temperatures as it occurs in Udimet 700, which is a nickel-base superalloy used extensively in turbine applications.

There has been extensive work[18-22] on Udimet 700 under low cycle fatigue in the temperature range of 25 to 926 °C although not much on fatigue crack growth. The alloy exhibited fatigue hardening behavior followed by fatigue softening at both 25 and 760 °C. At 760 °C and above, both environmental and creep effects become important as they appear to alter the mode of crack nucleation from transgranular to intergranular when frequency is reduced.[22] During the crack propagation stage, fracture was essentially transgranular with predominantly a faceted mode.

In our recent study[23] of fatigue crack growth in Udimet 700 using a fracture mechanics type of specimen, we found faceted growth even at a temperature as high as 850 °C. Furthermore, comparison of our data with room-temperature data[24] indicated a large effect of temperature on crack growth. It was not clear whether the effect of temperature was due to environmental interactions since the tests were done in air, or due to creep effects or to the inherent nature of the faceted mode of crack growth. The object of the present work was to investigate further the crack growth behavior of this alloy at room temperature and 850 °C in air and vacuum in order to determine the role of environment on the mode of crack growth and crack growth rates as well as the causes for the observed effect of temperature.

EXPERIMENTAL DETAILS

Compact tension specimens with nominal 1-T dimensions[25] but with 12.7 mm thickness were made from the same bar stock used earlier.[23] A standard duplex heat treatment was given the alloy with anneal at 1180 °C for 4 h, air cool, intermediate anneal at 1080 °C for 4 h, air cool, age at 845 °C for 24 h, furnace cool to 760 °C and age for 16-h and finally furnace cool

K. SADANANDA and P. SHAHINIAN are with the Thermostructural Materials Branch, Material Science and Technology Division, Naval Research Laboratory, Washington, DC 20375.

Manuscript submitted April 22, 1980.

to room temperature. Figure 1 shows the microstructure of the alloy after heat treatment. Extensive twinning characteristic of superalloys can be seen in the figure. That these twin boundaries form preferred sites for crack nucleation under fatigue has been shown earlier.[20]

All specimens were precracked at room temperature in air. All tests were performed on a servo-hydraulic machine at a frequency of 0.17 Hz with the specimen enclosed in a chamber for vacuum and heated by induction. A vacuum better than 1.33×10^{-4} Pa was obtained at the test temperature. Crack lengths were measured intermittently through a viewing port using a low magnification travelling microscope. Crack growth rates were determined from the plots of crack length *vs* time. Corrections to the crack lengths due to the initial curvature of the crack front were made from the fracture surface observations by averaging the crack lengths at 1/4, 1/2 and 3/4 positions of the specimen thickness. The stress intensity factor K, was calculated using the following relation[25] for $a/W \leq 0.7$

$$K = \frac{P}{B\sqrt{W}^{0.5}} [29.6(a/W)^{0.5} - 185.5(a/W)^{1.5} + 655.7(a/W)^{2.5} - 1017.0(a/W)^{3.5} + 638.9(a/W)^{4.5}] \quad [1]$$

and for $a/W > 0.7$ from the relation[26]

$$K = \frac{P}{2B}\left[\frac{W+a}{\sqrt{(W-a)}^{1.5}}\right]\left[4.0 + \frac{(W-a)}{(W+a)}\right] \quad [2]$$

where P is the applied load, a is the average crack length, W is the specimen width, and B is the thickness. The specimens were cycled until final failure. The vacuum crack growth data are compared with air data obtained earlier at 850 °C.

RESULTS

Environmental Effect

Figure 2 shows the crack growth rates, da/dN, as a function of ΔK at room temperature and 850 °C in air and vacuum. It has already been shown using several load amplitudes that crack growth under cyclic load can be adequately described by the linear elastic parameter, ΔK, even at 850 °C. Figure 2 also shows the room temperature data reported by Rau and Burke[24] for center cracked specimens of less than 1 mm thickness. Considering the significant difference in thickness and specimen geometry, both data agree well particularly at intermediate ΔK values.

Several observations can be made from the above figure. First, crack growth rates are higher in air than in vacuum at room temperature as well as at 850 °C. Enhanced crack growth rate in air even at room temperature was also observed in Alloy 718[27] and austenitic stainless steels.[28] These results together imply that it is erroneous[29] to attribute enhanced crack growth at high temperatures to purely environment, if vacuum data at high temperatures agree with air data at room temperature. In fact, Fig. 2 shows that for U dimet 700 the enhancement in crack growth rate due to environment is nearly the same at both temperatures. For example at $\Delta K = 40$ MPa $\sqrt{\text{m}}$, crack growth rates in air are nearly 2.5 times those in vacuum at both temperatures. In contrast the effect of environment on fatigue crack growth in Alloy 718 is significantly sensitive to temperature with growth rates at the same ΔK value being 5 to 10 times larger at 650 °C than at room temperature.[27] Thus for U dimet 700 the environmental interaction during fatigue is essentially an athermal process or process with very small activation energy, while for Alloy 718 it is a thermally activated process with an activation energy of the order of 30 kcal/mol.[28]

Most important to note in Fig. 2 is that temperature affects crack growth in U dimet 700 even in vacuum, and the effect is nearly the same in both air and vacuum.

Therefore, the increase in growth rate with temperature cannot be attributed to environment. Since creep becomes important at high temperatures, we shall next investigate if the temperature effect is due to the effect of creep.

Fig. 1 Microstructure of U dimet 700 (Etchant Kalling's reagent).

Creep Effect

To determine the contribution from creep the growth rates for fatigue in vacuum at 850 °C are compared with those for static load obtained earlier.[30,31] Figure 3 shows crack growth rates on a time basis da/dt (da/dt = $da/dN \times$ frequency) as a function of ΔK where ΔK for static load is the same as K_{max} the maximum stress intensity. Clearly, crack growth rates under cyclic loads are significantly higher than under static load. This implies that crack growth for fatigue is not due to a time-dependent process but is due to a cycle-dependent process. Also, note that the stress intensity required for time-dependent crack growth to occur at 850 °C is very high, of the order of 40 to 50 MPa $\sqrt{m}$. That is, for stress intensities at which fatigue crack growth occurs in vacuum at 850 °C, Fig. 2, little or no time-dependent contribution to crack growth is expected.

It could be argued that creep crack growth may not

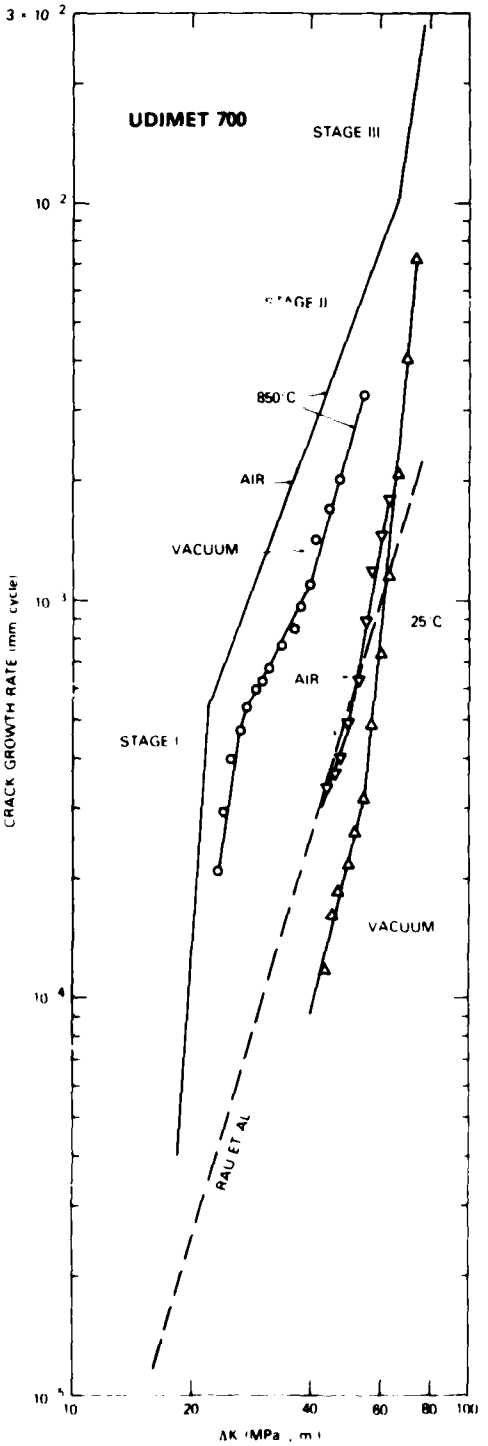

Fig. 2 Effect of environment and temperature on fatigue crack growth rate.

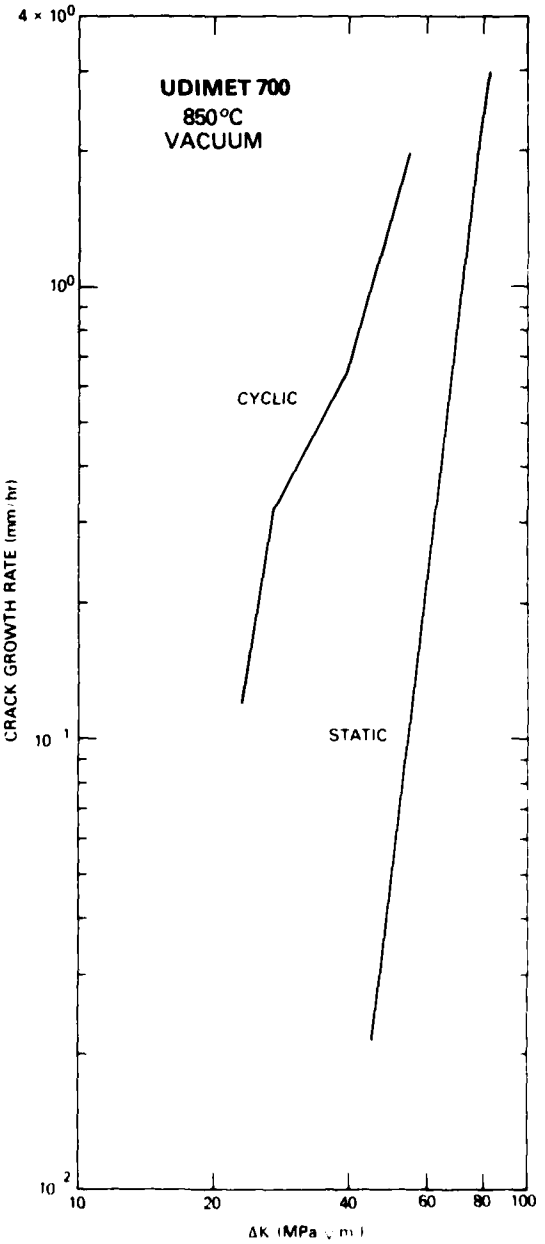

Fig. 3 Comparison of crack growth rates in vacuum under cyclic (0.17 Hz) and static loads.

occur for these stress intensities, but creep deformation may still occur which could influence the fatigue crack growth. However, our results[32] on the effects of superimposed hold period at the peak load in this alloy indicate that for stress intensities less than the threshold stress intensity for creep crack growth, creep deformation seems to retard fatigue crack growth by blunting the crack tip. Such retardation effects are not specific to Udimet 700 but were noticed in other alloy systems[33-36] with hold times or at low frequencies if stress intensities are less than the threshold stress intensities for creep crack growth. These results indicate that it is difficult to attribute the enhanced fatigue crack growth at high temperature directly to creep.

Modulus Effect

Since the effect of temperature on fatigue crack growth does not appear to be due to the two most commonly expected time-dependent contributions, *i.e.*, creep and environmental effects; the other possible causes could be the variation of elastic modulus or yield stress with temperature. That the elastic modulus is an important material property that controls fatigue crack growth was demonstrated earlier by several workers[37-39] and was also supported by theoretical analysis.[40] Speidel[39] obtained a good correlation of room temperature fatigue crack growth of several materials in vacuum when ΔK was normalized by modulus. Shahinian *et al*[41] suggested a possible correlation of crack growth variation with temperature by the modulus. Although normalization of high temperature crack growth data of several materials in air by their modulus brought the data closer to each other, correlation was very limited because of the superimposed environmental effects.[42] On the other hand, much better correlation of fatigue crack growth data in vacuum at several temperatures was obtained for Alloy 718[27] and Type 306 austenitic stainless steel.[28] It is of interest, therefore, to see how well the Udimet 700 data in vacuum could be correlated by elastic modulus.

Figure 4 shows crack growth rate, da/dN, as a function of $\Delta K/E$ where E, the elastic modulus for Udimet 700 is given as[43] 2.23×10^5 MPa and 1.69×10^5 MPa at 25 and 850 °C, respectively. Along with the Udimet data (solid lines), previously obtained data for Alloy 718[27] (dashed lines) and Type 316 stainless steel[28] (dotted line) are also represented for comparison. Clearly, there is no correlation of the Udimet data on a $\Delta K/E$ basis, although such correlation was observed for the other two alloys. But even for Alloy 718 and Type 316 stainless steel, data for both alloys do not fall on a single line unlike the case observed in other alloys at room temperature.[39] Speidel[39] deduced an empirical equation based on the correlation of data for several alloys at room temperature and is given by:

$$\frac{da}{dN} = 1.7 \times 10^{6}\left(\frac{\Delta K}{E}\right)^{3.5} \text{ m/cycle} \qquad [3]$$

which is also represented in Fig. 4 by the dash-dot line. The above line deviates from the data for Alloy 718 and Type 316 stainless steel. In fact, the form of the equation representing the data for Alloy 718 can be deduced as:

$$\frac{da}{dN} = 1.65 \times 10^{11}\left(\frac{\Delta K}{E}\right)^{4.9} \text{ m/cycle} \qquad [4]$$

The stainless steel data curve is very nearly parallel to the Alloy 718 data; and Eq. [2] is therefore valid for Type 316 stainless steel as well except for a change in the preexponent to 5.73×10^{11}.

For Udimet 700, it is clear that the enhanced crack growth at high temperature cannot be due directly to the variation of modulus. It is of interest to note in Fig. 4 however that Udimet 700 data at 25 °C coincides with Alloy 718 data up to $\Delta K/E$ value of 25×10^{-5} $\sqrt{\text{m}}$. At higher $\Delta K/E$ values crack growth rates for Udimet 700 are higher than those for Alloy 718.

Lack of correlation of crack growth data on a $\Delta K/E$

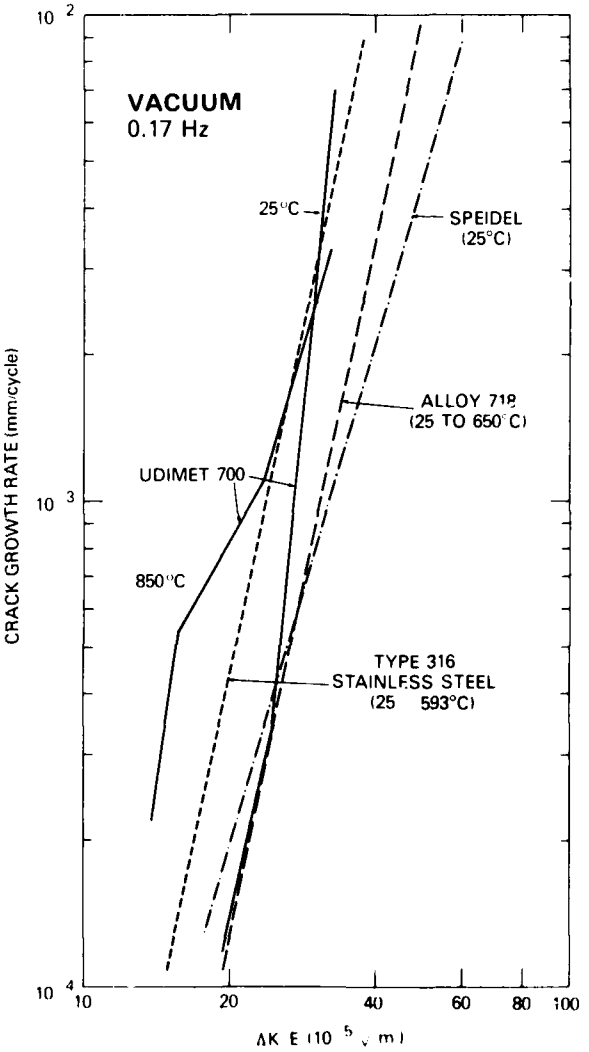

Fig. 4 Fatigue crack growth rates as a function of $\Delta K/E$ where E is the elastic modulus. Speidel curve corresponds to correlation of room temperature data of several materials.

basis may imply that such correlation may exist only for the striation mode of crack growth and not for the faceted mode as discussed by Speidel.[39] We can also rule out the variation of yield stress with temperature contributing directly to the observed effect of temperature on crack growth in Udimet 700, since yield stress decreases with temperature by less than a factor of two[43] (955 MPa at 25 °C and 690 MPa at 850 °C), while crack growth rate in Fig. 2 increases by nearly a factor of ten. Also, no correlation of growth rate with yield stress was observed for other alloys.[42] We shall next examine the fracture surface morphology for possible differences in crack growth at the two temperatures.

Fracture Surfaces

Figure 5 shows SEM observations of fracture surfaces of high temperature specimens in air and vacuum. Figure 5(*a*) in particular shows the faceted mode of crack growth in air where the arrows indicate the boundary between room temperature precrack and high temperature fatigue crack. All of the facets are covered with an oxide layer as can be seen at the higher magnification in Fig. 5(*b*). From the crystalline nature of the oxide phase, and from the detailed analysis[44] of the sequence of gas-alloy reactions at high temperature, the oxidation product on the surface is likely to be either Al_2O_3 or a spinel. That the oxide formed subsequent to crack growth rather than during crack growth is evident since the volume of the oxide particles is significantly reduced with increase in crack length or with the decrease in the duration of exposure of the freshly created surface at the test temperature. Crack growth in air[23] was essentially by the faceted mode except at high ΔK values corresponding to Stage III where some superimposed intergranular growth also occured. Since the stress intensities corresponding to Stage III are in the range where creep crack growth is expected, the onset of the intergranular growth was attributed to the superimposed creep effects.

The surface of the vacuum specimen tested at 850 °C is shown in Figs. 5(*c*) through (*e*). The faceted mode can be seen clearly in Fig. 5(*c*) which corresponds to the region close to the precrack. Under higher magnifi-

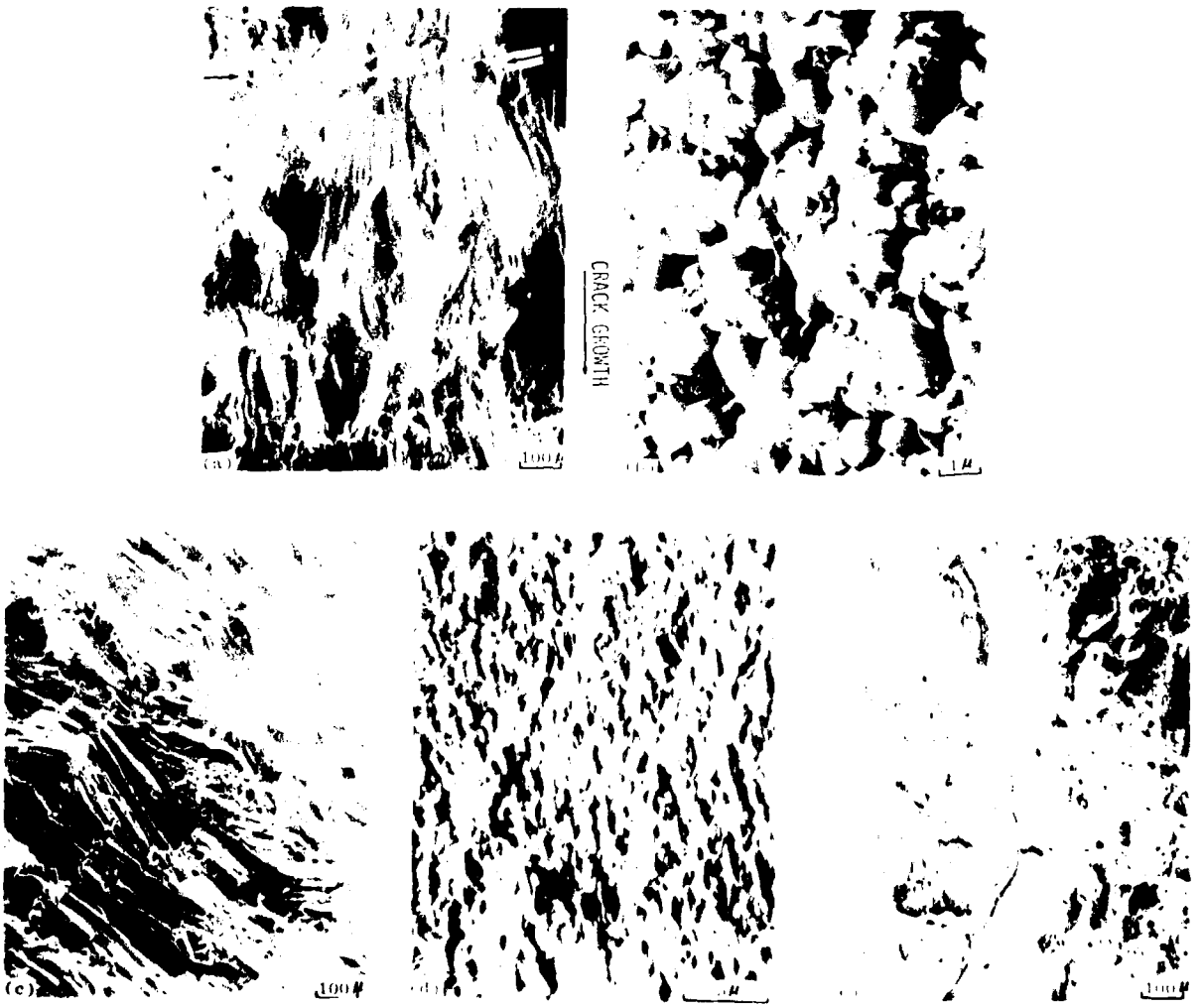

Fig. 5 SEM observations of fracture surfaces of high temperature specimens (*a*) and (*b*) in air and (*c*) (*d*) and (*e*) in vacuum.

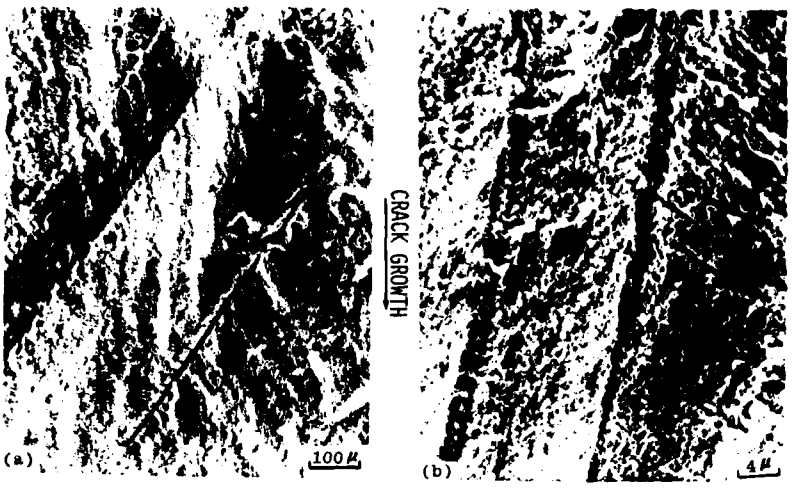

Fig. 6— Fracture surface of room temperature specimen (*a*) secondary cracks along the twin interface, (*b*) secondary cracks at an angle to the twin interfaces.

cation, particles can be seen on the fracture surface in Fig. 5(*d*) which may not be oxidation products since these were also seen in a vacuum specimen tested at room temperature. At low stress intensity the fracture surface is almost entirely covered with facets. With increase in stress intensity there is a decrease in the size of the facets to the extent that at the high ΔK region the surfaces are covered with irregular lines, Fig. 5(*e*), indicative of significant plastic deformation. Between these lines the faceted growth can still be noticed. There was however no noticeable evidence of striations characteristic of the ductile mode of crack growth, and overall growth occurred only by the faceted mode.

At the outset there appears to be no difference in the fracture surface morphology as a function of temperature or environment. Attempts to identify the plane of facets were unsuccessful because of the small size of the facets. To examine the fracture mode in detail the fracture surfaces were etched with Kalling's reagent and then examined. Figure 6 shows some interesting features associated with the fracture surfaces of room temperature specimens. Square-shaped γ' precipitates were observed on all of the facets. In general, there is no difference in the etched surfaces in terms of environment at both temperatures. However, there is a noticeable difference in terms of temperature. Most importantly, there is extensive secondary cracks on the facets which were not seen in the high temperature specimens. In some cases these cracks are seen along the twin boundary interfaces particularly when the twin interfaces are at an angle to the direction of crack growth, such as in Fig. 6(*a*). Notice the absence of cracks along the twin interfaces in Fig. 6(*b*) since the direction of the crack growth is nearly parallel to the twin orientation. For this case, the secondary cracks, however, are still seen but they are at an angle to the twins. Examination of the surface normal to the fracture surface showed that none of these cracks extend deep into the grains. Also, the average spacing between the secondary cracks was found to be much smaller than the crack length increment per cycle. Examination of the mating surfaces revealed that these secondary cracks are present on both halves of the fracture surfaces.

The shape of the γ' precipitates, the twin boundary orientation and the orientation of the secondary cracks can be used to determine the orientation of the facets in Udimet 700. Based on the precipitate shape and their distribution on the fracture surface, we show in the following that the plane of the facet is likely to be a cleavage plane rather than a slip plane. This will be further confirmed by using the orientation relationships between the twin boundaries, cracks and the precipitates. It has been well established[45-47] for this alloy that the growth of γ' precipitates during aging occurs in crystallographically, well-defined directions. They tend to form mostly in cubic orientations with cube planes of the precipitates parallel to the cube planes of the matrix, thus, forming a coherent precipitate. Furthermore, the distribution of the precipitates is such as to align them along cube directions. Since the slip planes for nickel

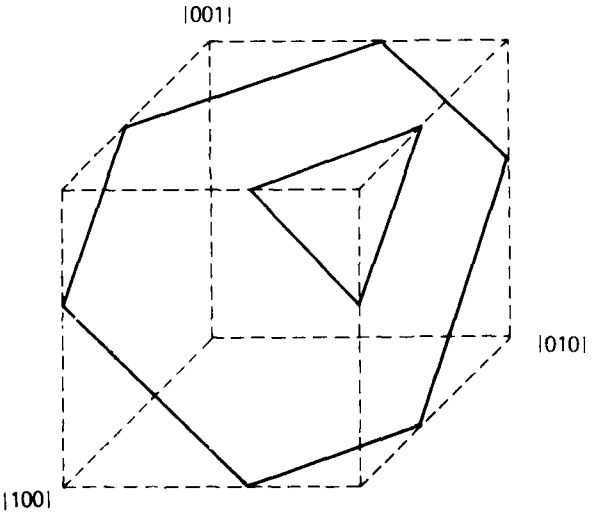

Fig. 7 The expected shape of the γ' precipitates on the fracture surface if the faceted plane is a slip plane.

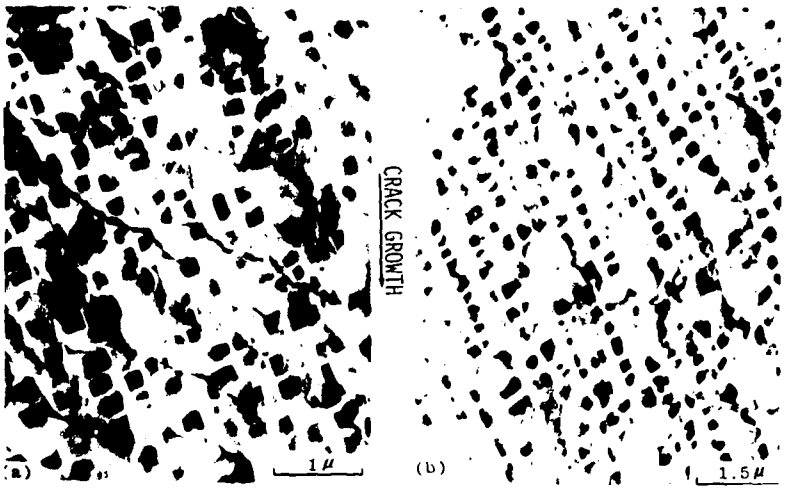

Fig. 8—Shape of the precipitates on the fracture surfaces at (*a*) room temperature and (*b*) at 850 °C.

base superalloys are generally restricted to {111} planes, facet orientation along a slip plane would cut the precipitates along a {111} plane which would reveal the precipitates as either triangular shaped, or regular or irregular hexagonal shaped as shown in Fig. 7. The shape of the precipitates observed on the etched fracture surface can be more clearly seen under higher magnification in Fig. 8. The square shaped precipitates aligned along cube directions indicate, therefore, that the plane of the facets is more likely to be a {100} plane, both at room temperature, Fig. 8(*a*), and at 850 °C, Fig 8(*b*).

Orientation of the facets can be confirmed by trace analysis of the twin boundary and of the secondary cracks in Fig. 6(*b*). For this we use the angles between the twin boundary and the edges of the precipitates, between the twin boundary and the cracks, and finally between the cracks and edges of the precipitates. It is known[48] that the twinning in fcc materials occurs along {111} planes which make a {110} trace on a {100} plane. Indeed, the angle between the edges of the precipitates and the twin boundary is close to 45 ° corresponding to the angle between ⟨110⟩ and ⟨100⟩ directions. Assuming the secondary cracks on the facets are slip line cracks with the slip plane parallel to the {111} plane, the trace of the cracks would also be along the ⟨110⟩ direction. The angle between the twin boundary and the average orientation of the cracks is nearly equal to 70 °, which is close to the angle between two ⟨110⟩ directions. Finally, the average angle between the cube edges of the precipitates and the slip line cracks in Fig. 8(*a*) is also close to 45 ° confirming the two directions as ⟨100⟩ and ⟨110⟩, respectively. All of the measured angles are within ± 10 deg from the expected angles, and this is reasonable[13] since the plane of the facets is not necessarily normal to the beam. All of the above angular relationships are satisfied only if the facet is parallel to the {100} plane which is a cleavage plane rather than the slip plane of the alloy.

In contrast to room temperature fracture, the high temperature facets do not show any extensive secondary cracks on the surface. Square shaped precipitates aligned along the cube directions, Fig. 8(*b*), however, indicate that the faceted growth occurs along {100} plane similar to that at room temperature. Although crack growth occurs along a specific plane in each grain, the average orientation of the crack remains normal to the stress axis. Also on most of the facets river lines characteristic of cleavage could be noticed.

DISCUSSION

Detailed fracture surface analysis indicates that faceted mode of fatigue crack growth occurs in Udimet 700 along {100} cleavage planes, rather than {111} slip planes. Change in the temperature or environment has no effect on the mode of crack growth. Gell and Leverant[8] on the other hand, observed the faceted mode of crack growth in Mar-M 200 alloy along {111} planes. Their analysis, however, pertains to unnotched specimens with large grain size. This difference in the orientation of the facets can be due to the difference in materials, specimen geometry or in the test conditions. Note that crack growth rates at room temperature are reasonably close to room temperature data reported by Rau *et al.*[24] These authors also observed faceted crack growth in Udimet 700; however, there was no explicit determination of the plane of the facets. They observed that the crack initiates along a slip plane 45 ° to the tensile axis but soon changes to normal to the stress axis.

While faceted crack growth is generally assumed to be along a slip plane similar to the crystallographic Stage I mode of crack growth, several observations indicate that it need not be so. Meyn[10] observed that faceted growth in an aluminum alloy occurs along {100} plane in air while along the {100} or {111} plane in vacuum. On the other hand, in Ti-alloys[11,12] faceted growth has been reported along basal planes or close to the basal planes, which are cleavage planes. As in Udimet 700, Yoder *et al*[12] have observed the presence of a significant number of secondary cracks which are claimed to be slip band cracks on the fracture surface. Richards[4] has shown with reference to Fe-Si single crystals that the plane of crack growth would also depend on the symmetry of the slip systems in relation

to the crack plane. From the above discussion, we conclude that the observation of crystallographic fatigue crack growth long {100} cleavage planes is not specific to Udimet 700 and in general, the faceted mode of crack growth can occur either along slip planes or along cleavage planes. The implication of this in terms of a fatigue crack growth model is discussed in a subsequent paper.

Except for the observation of the secondary cracks on the facets there is no other difference in the crack growth mode at 25 and 850 °C. Other factors such as environment, creep, variation in modulus or yield strength do not appear to be directly responsible for the observed temperature effect. It seem logical, therefore, to attribute the temperature effect to the case of secondary cracking at room temperature. Formation of these cracks decreases the stress intensity at the crack tip and, thus, lowers the growth rate. Since the precipitates form more effective barriers for slip at room temperature, the slip gets concentrated close to the crack tip which helps in the nucleation of the secondary cracks. Such formation of secondary cracks along slip planes at room temperature has been observed also in other alloys.

The difficulty with the above explanation is that it attributes the observed temperature effect in Udimet 700 to lower crack growth rates at room temperature; but the growth rates of the alloy at room temperature fall reasonably close to the rates for other high strength alloys,[42] whereas the growth rates at high temperature appear to be abnormally high. It is possible that secondary cracking may also occur at room temperature in other alloys, but this has to be ascertained by using specimens tested in vacuum since some of these alloys are very sensitive to environment. In a subsequent paper the mechanism of the faceted mode of crack growth in high strength alloys is examined in relation to the existing models of fatigue crack growth.

SUMMARY AND CONCLUSIONS

Fatigue crack growth behavior in Udimet 700, a nickel-base superalloy, was examined in detail. Crack growth rates were determined in air and vacuum at room temperature and 850 °C at 0.17 Hz. Crack growth rates increased by nearly an order of magnitude with increase in temperature from 25 to 850 °C, and the increase was the same in air and vacuum. Therefore, the effect of environment remained nearly the same at both temperatures. The analysis shows that the increased growth rates with increase in temperature are unlikely to be due to an environmental effect, creep effect or variation of elastic modulus with temperature.

Fracture surfaces were examined under SEM in both etched and unetched conditions. Crack growth occurred by a faceted mode in both air and vacuum at both 25 and 850 °C. From the fractographic analysis it was concluded that the faceted growth occurred on cleavage planes rather than on slip planes for all the test conditions. There was significant secondary cracking at room temperature compared to that at 850 °C, and this may be responsible for the observed effect of temperature on crack growth. The occurrence of secondary cracking at room temperature was attributed to the difficulty of slip at room temperature in the precipitation hardened alloy.

ACKNOWLEDGMENTS

The present research effort was supported by the Office of Naval Research. The authors acknowledge helpful discussions with D. A. Meyn and G. R. Yoder of the Naval Research Laboratory.

REFERENCES

1. P. J. E. Forsyth: *Proceedings of the Symposium on Crack Propagation*, Cranfield, The College of Aeronautics, 1962, vol. 1, pp. 76–94.
2. R. P. Wei: *Trans. ASM*, 1967, vol. 60, p. 279.
3. K. R. L. Thompson and J. V. Craig: *Met. Trans.*, 1970, vol. 1, pp. 1047–49.
4. C. E. Richards: *Acta Metall.*, 1971, vol. 19, p. 583.
5. G. C. Garrett and J. F. Knott: *Acta Metall.*, 1975, vol. 23, pp. 841–48.
6. R. N. Wright and A. S. Argon: *Met. Trans.*, 1970, vol. 1, p. 3065.
7. J. C. Chesnutt, C.G. Rhodes and J. C. Williams: ASTM STP 600, C. D. Beachem and W. R. Warke, eds., American Society for Testing and Materials, pp. 99 138, Philadelphia, 1976.
8. M. Gell and G. R. Leverant: *Acta Metall.*, 1968, vol. 16, pp. 533–61.
9. D. J. Duquette, M. Gell, and J. W. Piteo: *Met. Trans.*, 1970, vol. 1, pp. 3107–15.
10. D. A. Meyn: *Trans. ASM*, 1968, vol. 61, pp. 52–61.
11. D. A. Meyn: *Met. Trans.*, 1971, vol. 2, pp.853–65.
12. G. R. Yoder, L. A. Cooley, and T. W. Crooker: *Met. Trans. A*, 1977, vol. 8A, pp. 1737–43.
13. D. Eylon: *Met. Trans. A*, 1979, vol. 10A, pp. 311–17.
14. R. W. Hertzberg and W. J. Mills: ASTM-STP 600, C. D. Beachem and W. R. Warke, eds., American Society for Testing and Materials, pp. 220–34, 1976.
15. A. Yuen, A. W. Hopkins, G. R. Leverant, and C. A. Rau: *Met. Trans.*, 1974, vol. 5, pp.1833–42.
16. H. D. Williams and G. C. Smith: *Philos. Mag.*, 1965, vol. 13, p. 835.
17. J. L. Robinson and C. J. Beevers: *Met. Sci. J.*, 1973, vol. 7, p. 135.
18. C. H. Wells and C. P. Sullivan: *Trans. ASM*, 1964, vol. 57, pp. 841–55.
19. C. H. Wells and C. P. Sullivan: *Trans. ASM*, 1965, vol. 58, pp. 391–402.
20. C. H. Wells and C. P. Sullivan: *Trans. ASM*, 1967, vol. 60, pp. 217–22.
21. C. H. Wells and C. P. Sullivan: *Trans. ASM*, 1968, vol. 61, pp. 149–55.
22. F. E. Organ and M. Gell: *Met. Trans.*, 1971, vol. 2, pp. 943–51.
23. K. Sadananda and P. Shahinian: *Eng. Fract. Mech.*, 1979, vol.11, pp. 73–86.
24. C. A. Rau, Jr. and L. H. Burke: *Eng. Fract. Mech.*, 1971, vol. 12, pp. 211–22.
25. *Plane-Strain Fracture Toughness of Metallic Materials*: E399–74, Annual Book of ASTM Standards, Part II, pp. 432–51, 1974.
26. W. K. Wilson: *Eng. Fract. Mech.*, 1976, vol.2, p. 169.
27. P. Shahinian and K. Sadananda: *Engineering Aspects of Creep*, Inst. Mech. Engrs., London, vol. 2, pp. 1–7, 1980.
28. K. Sadananda and P. Shahinian: *Met. Trans.*, 1980 vol. 11A, pp. 267–76.
29. L. A. James: *J. Eng. Mater. Technol.*, 1976, vol. 98, pp. 235–38.
30. K. Sadananda and P. Shahinian: *Mater. Sci. Eng.*, 1980, vol. 43, pp. 159–68.
31. K. Sadananda and P. Shahinian: *Met. Trans. A*, 1978, vol. 9A, pp. 79–84.
32. K. Sadananda and P. Shahinian: *J. Mater. Sci.*, 1978, vol. 13, pp. 2347–57.
33. P. Shahinian and K. Sadananda: *J. Eng. Mater. Technol., Trans. ASME*, 1979, vol. 101, pp. 224–30.

34. P. Shahinian and K. Sadananda: *Symposium on Creep-Fatigue Interaction, ASME MPC-3*, pp. 365–90, American Society of Mechanical Engineers, New York, 1976.
35. J. R. Haigh: *Eng. Fract. Mech.*, 1975, vol. 7, pp. 271–84.
36. R. B. Scarlin: *Met. Trans. A*, 1977, vol. 8A, pp. 1941–48.
37. S. Pearson: *Nature*, 1966, vol. 211, pp. 1077–78.
38. R. C. Bates and W. G. Clark, Jr.: Sci. Paper 68-1-D7-RDAFC-P1, Westinghouse Research Laboratories, September 1968.
39. M. O. Speidel: *High Temperature Materials in Gas Turbines*, P. R. Sahm and M. O. Speidel, eds., pp. 207–51, Elsevier, Amsterdam, 1974.
40. K. Sadananda and P. Shahinian: *Int. J. Fract.*, 1977, vol. 13, pp. 585–94.
41. P. Shahinian, H. H. Smith, and H. E. Watson: *J. Eng. Ind., (Trans. ASME, B)*, 1971, vol. 93, pp. 976–80.
42. P. Shahinian: *Met. Technol.*, 1978, vol. 5, no. 11, pp. 372–80.
43. "High Temperature High Strength Nickel Base Alloys," International Nickel Company, Inc., Huntington, WV, 1964.
44. F. S. Pettit and J. K. Tien: *Corrosion Fatigue: Chemistry, Mechanics and Microstructure*, O. F. Devereux, A. J. McEvily, and R. W. Staehle, eds., pp. 576–89, National Association of Corrosion Engineers, Houston, TX, 1972.
45. Y. A. Bagaryatski and Y. D. Tiapkin: *Sov. Phys. Cryst.*, 1957, vol. 2, p. 414, also 1961, vol. 5 p. 842.
46. C. Buckle, B. Genty, and J. Manene: *Rev. Met.*, 1959, vol. 56, p. 247.
47. A. J. Ardel and R. B. Nicholson: *Acta Metall.*, 1966, vol. 14, pp. 1295–1309.
48. R. J. De Angelis and J. B. Cohen: *Deformation Twinning*, R. E. Red-Hill, J. P. Hirth, and H. C. Rogers, eds., pp. 430–64, Gordon and Breach Science Publishers, NY, 1964.